

New Extended Rayleigh Distribution: Properties, Estimation, Simulation and Application

Ifeanyi C. Anabike¹, Ebube S. Okoro², Chinyere P. Igbokwe³, Precious O. Ibeakuzie⁴,
and Divine-Favour N. Ekemezie⁵

^{1,2,4, 5}Department of Statistics, Faculty of Physical Sciences, Nnamdi Azikiwe
University, Awka, Nigeria

³Department of Statistics. Abia State Polytechnic, Aba, Nigeria

Corresponding Author: Divine-Favour N. Ekemezie ; email: de.ngozi@stu.unizik.edu.ng

Abstract

In this study, the New Extended Rayleigh (NER) distribution which was developed from the New Extended-X family of distributions. It was designed to have a better fit for modeling real life events. Few works on Rayleigh distribution were captured. Further into this paper, mathematical properties such as moment, mean and quantile function were studied. Through two- and three-dimensional plots of the probability density function, hazard rate, mean, skewness, kurtosis, and variance the flexibility of the proposed model was proved. MCMC simulation studies for the non-Bayesian and Bayesian methods were conducted at different samples sizes and initial parameter values and the results proved that the distribution is robust. The model was implemented to real life data and the results showed competitiveness with existing distributions.

Keywords— New Extended Rayleigh distribution; New Extended-X family of distributions; Rayleigh distribution, Simulation.

1 Introduction

The creation of new probability distributions by several researchers are a significant approach to model the likelihood of different outcomes in uncertain situations, decision making, as well as giving an assistance to underpin several statistical tests and confidence interval decisions and a whole bunch of others see, Maurya et al. [20], Badr, Badawi, Alzubidi, et al. [7]. In order to ascertain a more distinguished probability distribution, the exemplary resolve is to introduce additional parameters to existing distributions or exponentiate or by adding baseline (traditional) distributions to families of distributions reference Tekle, Roozegar, and Bidram [41]. The writers' interest is to present a more flexible probability distribution by introducing a traditional distribution to a family of distributions. This was achieved using the Rayleigh distribution named after Lord Rayleigh Reid [36], having its probability density function (p.d.f) and cumulative distribution function (c.d.f) as

$$g(x, \delta) = \frac{x}{\delta^2} e^{-\frac{x^2}{\delta^2}}; \quad \delta > 0, x > 0, \quad (1)$$

and

$$G(x, \delta) = 1 - e^{-\frac{x^2}{\delta^2}}, \quad (2)$$

respectively.

The Rayleigh distribution is characterized by its simple yet effective probability density and cumulative distribution functions, is widely utilized for modeling continuous non-negative variables in various disciplines. Its applications span across engineering, where it accurately models phenomena like signal strengths and noise

levels, to medical research, where it fits particle size distributions in pharmaceuticals. The distribution's adaptability is further demonstrated through extensions like the Weibull Rayleigh distribution, which introduces additional parameters to tailor its shape to specific data patterns [21]. Such advancements underscore its significance in statistical modeling and its continual evolution to address diverse analytical needs in fields requiring robust probabilistic tools. The Rayleigh distribution thus stands as a cornerstone in probabilistic modeling, continuously refined to meet the demands of modern scientific inquiry.

The non negativity of random variables is crucial for implementing and analyzing probability models and the Rayleigh distribution is a continuous probability for such variables. The pivotal essence of the Rayleigh distribution cannot go unnoticed, having the ability to model real-time data in medical fields, engineering fields, and applied statistics. As a result of this, a substantial amount of researchers have piqued interest in developing the Rayleigh distribution. Ateeq, Qasim, and Alvi [6] studied An extension of Rayleigh distribution and applications where simulations and estimations of the parameters were performed including modelling to real-life data sets. Weibull Rayleigh distribution, a three parameter distribution was postulated by Merovci and Elbatal [21], having a p.d.f that assumes a bathtub shape and observed to be positively skewed. The statistical properties, Maximum likelihood estimations (MLE) were conducted as well. Ahmad, Ahmad, and Ahmed [2] worked on Transmuted inverse Rayleigh distribution: A generalization of the inverse Rayleigh distribution. Bhat and Ahmad [8] introduced a new generalization of Rayleigh distribution properties and application. Soliman, Amin, and Abd-El Aziz [38] worked on Estimation and prediction from inverse Rayleigh distribution based on lower record values, Ahmed, Nofal, Abd El Hadi, et al. [3] studied Exponentiated transmuted generalized Raleigh distribution: A new four parameter Rayleigh distribution, Kilai et al. [19] applied the Rayleigh distribution to the medical field where he introduced A new versatile modification of the Rayleigh distribution for modeling COVID-19 mortality rates. The application of the Rayleigh distribution in the engineering field was demonstrated by Rao and Mbwanbo [35]. These are but a few works that inculcated the utilization of the Rayleigh distribution. Meanwhile, there are other interesting distributions, see [26, 13, 30, 23, 14, 18, 17, 11, 24, 25, 27, 16, 31, 33, 15, 28, 34, 10, 42, 32, 22, 1] for details.

The family of distributions that was used to further modify the Rayleigh distribution in this work introduced by Zichuan et al. [45] is A New Extended-X (NE-X) family of Distributions having a c.d.f and p.d.f as

$$G(x; \sigma, \delta) = 1 - \left\{ \frac{1 - F(x; \delta)^2}{1 - (1 - \sigma) 1 - F(x; \delta)^2} \right\}^\delta; \quad \sigma > 0, \quad x \in \mathbb{R} \quad (3)$$

and

$$g(x; \sigma, \delta) = \frac{2\sigma^2 F(x; \delta) \left\{ 1 - F(x; \delta)^2 \right\}^{\sigma-1}}{\left\{ 1 - (1 - \sigma) F(x; \delta)^2 \right\}^{\sigma+1}}; \quad x \in \mathbb{R} \quad (4)$$

respectively.

This family of distributions was created to yield more flexible probability distributions. It extends any baseline distribution by introducing an additional parameter which serves as a scale as well as a shape parameter and provides greater accuracy in fitting real-life data. The writers further worked on a sub-model which they named a New Extended Weibull (NEW) distribution. The c.d.f, p.d.f, hazard function and other mathematical properties were discussed (with plots shown where necessary). With the aid of two data sets, the distribution was utilized to model data and the results show that the novel distribution performed better than the competitive distributions. The significance of the study of the NE-X family was initially accomplished in the financial science but later discovered to be an efficient use in the engineering and medical sciences. Alamri et al. [4] used the NE-X family to model the COVID 19 mortality rate in Saudi Arabia where the length-biased exponential distribution was introduced to the family. The p.d.f having different shapes shows the true flexibility of the NE-X family.

To generate the novel distribution here, we insert equation 1 and equation 2 into equation 3 and equation 4 giving us a c.d.f of

$$G(x; \theta, \lambda) = 1 - \left\{ \frac{1 - \left(1 - e^{-\frac{x^2}{2\lambda^2}} \right)^2}{1 - (1 - \theta) \left(1 - e^{-\frac{x^2}{2\lambda^2}} \right)^2} \right\}^\theta \quad (5)$$

and a p.d.f of

$$f(x; \theta, \lambda) = \frac{2\theta^2 \frac{x}{\lambda^2} e^{-\frac{x^2}{2\lambda^2}} \left(1 - e^{-\frac{x^2}{2\lambda^2}}\right) \left\{1 - \left(1 - e^{-\frac{x^2}{2\lambda^2}}\right)^2\right\}^{\theta-1}}{\left[1 - (1 - \theta) \left(1 - e^{-\frac{x^2}{2\lambda^2}}\right)^2\right]^{\theta+1}} \quad (6)$$

Survival function which is the function that gives the probability that a patient or any other object of interest can survive a certain time(t). For the NER distribution, it is presented as

$$s(x) = \left\{ \frac{1 - \left(1 - e^{-\frac{x^2}{2\lambda^2}}\right)^2}{1 - (1 - \theta) \left(1 - e^{-\frac{x^2}{2\lambda^2}}\right)^2} \right\}^{\theta}. \quad (7)$$

Hazard rate is defined as the probability that a certain object will survive a particular time given an initial survival rate. It is mathematically derived by dividing the p.d.f by the survival rate. The hazard rate of HOER is given thus;

$$h(x) = \frac{2\theta^2 \frac{x}{\lambda^2} e^{-\frac{x^2}{2\lambda^2}} \left(1 - e^{-\frac{x^2}{2\lambda^2}}\right)}{\left[1 - (1 - \theta) \left(1 - e^{-\frac{x^2}{2\lambda^2}}\right)^2\right] \left[1 - \left(1 - e^{-\frac{x^2}{2\lambda^2}}\right)^2\right]}. \quad (8)$$

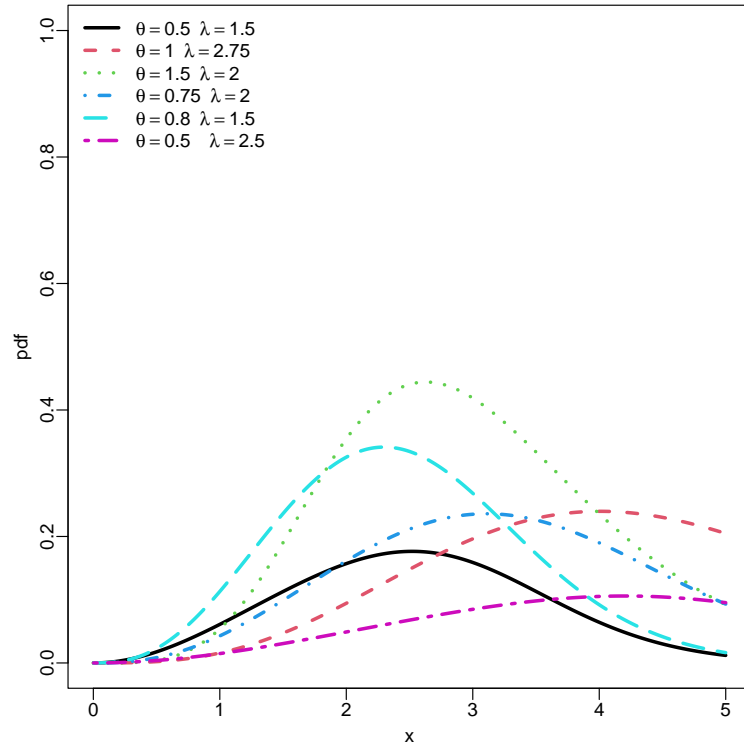


Figure 1: p.d.f of NER (θ, λ)

Figure 1 illustrates the p.d.f of the NER distribution at varying randomly selected parameter values of both the shape and scale parameters. The display shows the p.d.f has a reverse bathtub shape, strictly increasing and is right-tailed. Figure 2 is the 3D plot of the p.d.f.

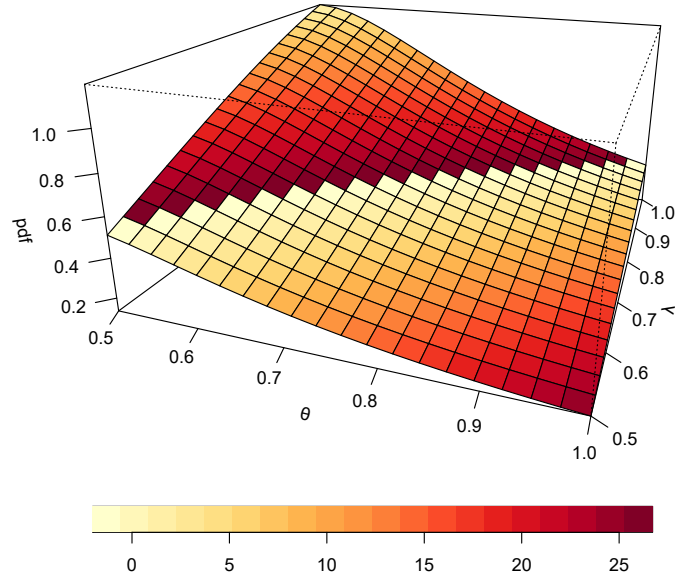


Figure 2: 3D p.d.f of NER (θ, λ)

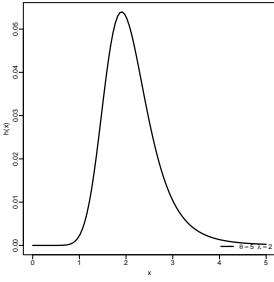


Figure 3: hazard function of NER (θ, λ)

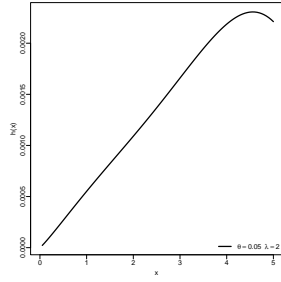


Figure 4: hazard function of NER (θ, λ)

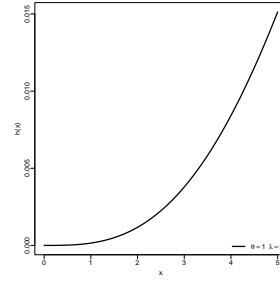


Figure 5: hazard function of NER (θ, λ)

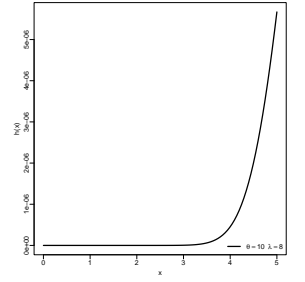


Figure 6: hazard function of NER (θ, λ)

In figures 3, 4, 5 and 6 which represents various forms of the hazard function of the distribution, evidently show a reversed bath-tub shape, strictly increasing, and j-shapes. There is a noticeable difference between the p.d.f plots and those of the hrf.

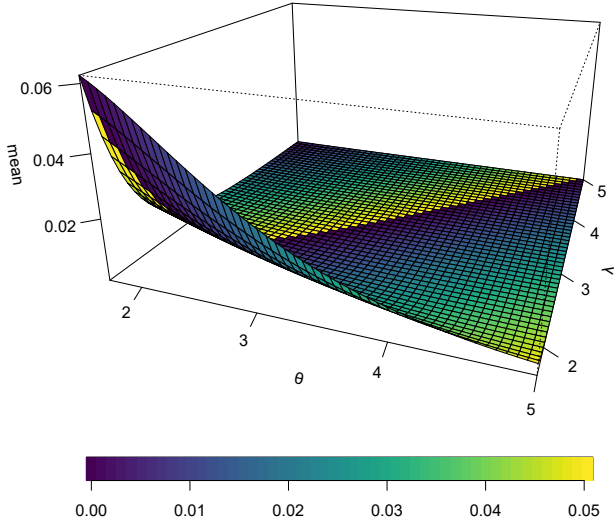


Figure 7: mean function of NER (θ, λ)

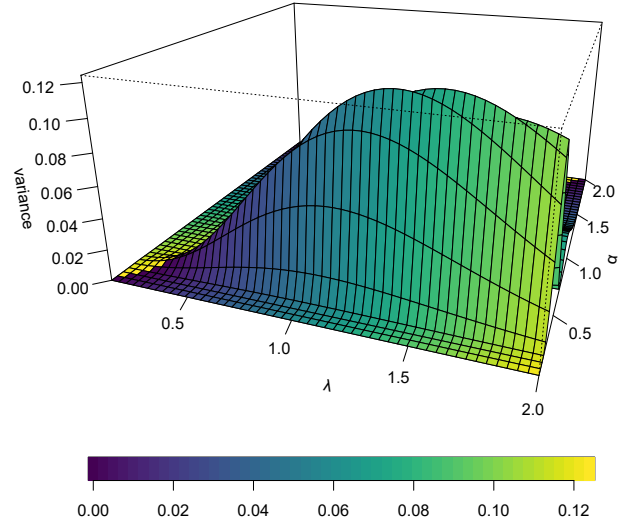


Figure 8: variance of NER (θ, λ)

Figures 7, 8 are the shapes of the mean and variance in 3D. It can be seen in figure 8 that θ as the values are increasing, curves are formed until it reaches the maximum value where it flattens, this elaborates on the ability for a parameter in the distribution to act as both a scale and shape.

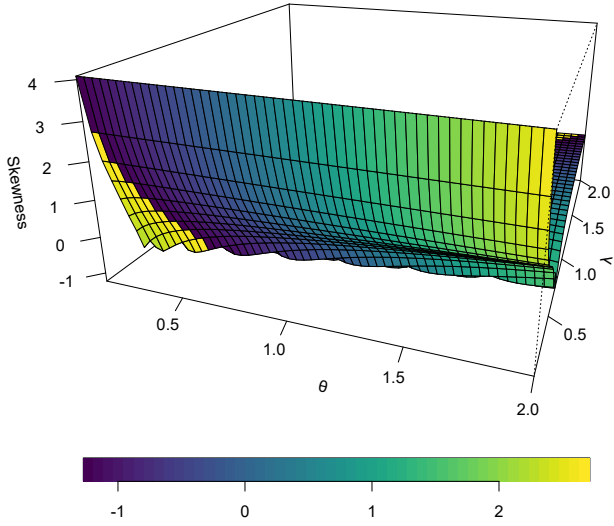


Figure 9: skewness of NER (θ, λ)

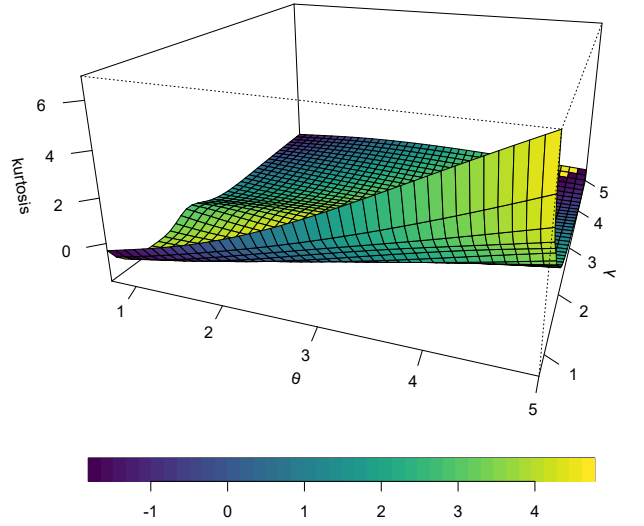


Figure 10: kurtosis of NER (θ, λ)

Figures 9 and 10 are the 3D plots of the skewness and kurtosis respectively.

2 Properties

In this section, some properties of the proposed model are discussed.

2.1 Moment

Let X be a random variable which follows the $\text{NER}(\theta, \lambda)$, the r th crude moment represented as μ_r' is

$$\begin{aligned}\mu_r' &= E(x^r) = \int_0^\infty x^r f(x) dx \\ &= \frac{2\theta^2}{\lambda^2} \sum_{i,j,k,l=0}^\infty (-1)^{i+j+k+l} \binom{\theta-1}{i} \binom{\theta+j}{j} \binom{2i+2j+1}{k} \binom{j}{l} \frac{\theta^l 2^{\frac{r}{2}} \lambda^{r+2}}{(1+k)^{\frac{r}{2}+1}} \Gamma\left(\frac{r}{2}+1\right)\end{aligned}\quad (9)$$

2.2 Mean

To generate the mean, we equate $r = 1$ in equation 9 and obtain

$$\mu_1' = \frac{2\theta^2}{\lambda^2} \sum_{i,j,k,l=0}^\infty (-1)^{i+j+k+l} \binom{\theta-1}{i} \binom{\theta+j}{j} \binom{2i+2j+1}{k} \binom{j}{l} \frac{\theta^l 2^{\frac{1}{2}} \lambda^3}{(1+k)^{\frac{1}{2}+1}} \Gamma\left(\frac{1}{2}+1\right) \quad (10)$$

2.3 Quantile Function

In probability and statistics, the quantile function determines the value of a random variable corresponding to a specified probability input. Essentially, it quantifies the probability that a random variable will fall within a given range or below a certain probability value for a specific probability distribution. Additionally, it is referred to as the percentile function, percent-point function, or inverse cumulative distribution function, derived from the cumulative distribution function (c.d.f) or simply inverse distribution function. To obtain this let's equate $u = F(x)$ so that we have;

$$u = 1 - \left\{ \frac{1 - \left(1 - e^{-\frac{x^2}{2\lambda^2}}\right)^2}{1 - (1 - \theta) \left(1 - e^{-\frac{x^2}{2\lambda^2}}\right)^2} \right\}. \quad (11)$$

Further expansion will lead to

$$Q(u) = \lambda \left[2 \ln \left\{ \frac{1 - (1 - \theta^2) (1 - u)^{\frac{1}{\theta}}}{2[1 - (1 - \theta) (1 - u)^{\frac{1}{\theta}}]} \right\} \right]^{\frac{1}{2}}. \quad (12)$$

3 Point Estimation

Here, we study some non-bayesian and bayesian estimation estimation procedures. The non-bayesian methods considered are the maximum likelihood, the least squares method, the maximum product spacing, the weighted least squares, the cramer von mises method, the Anderson-Darling method and the right-tailed Anderson-Darling method. Under the Bayesian estimation, we consider the Squared error loss function, the Linear-exponential loss function and the generalized entropy loss function.

3.1 Maximum Likelihood Estimation

Let x_1, x_2, \dots, x_n be random sample of size n obtained from NER distribution, the likelihood of ξ being its vector of parameters can be written as

$$L(x_i; \xi) = \frac{2^n \theta^{2n}}{\lambda^{2n}} e^{-\frac{\sum_{i=1}^n x_i^2}{2\lambda^2}} \prod_{i=1}^n \left(1 - e^{-\frac{x_i^2}{2\lambda^2}}\right) \left\{1 - \left(1 - e^{-\frac{x_i^2}{2\lambda^2}}\right)^2\right\}^{\theta-1} \left[1 - (1 - \theta) \left(1 - e^{-\frac{x_i^2}{2\lambda^2}}\right)^2\right]^{-(\theta+1)} \quad (13)$$

The log-likelihood is

$$\begin{aligned} \ell = \ln L(x_i; \xi) &= n \ln 2 + 2n \ln \theta - 2n \ln \lambda - \frac{\sum_{i=1}^n x_i^2}{2\lambda^2} + \sum_{i=1}^n \ln \left(1 - e^{-\frac{x_i^2}{2\lambda^2}} \right) \\ &+ (\theta - 1) \sum_{i=1}^n \ln \left\{ 1 - \left(1 - e^{-\frac{x_i^2}{2\lambda^2}} \right)^2 \right\} - (\theta + 1) \sum_{i=1}^n \ln \left[1 - (1 - \theta) \left(1 - e^{-\frac{x_i^2}{2\lambda^2}} \right)^2 \right] \end{aligned} \quad (14)$$

The partial derivative with respect to θ and λ are respectively

$$\begin{aligned} \frac{\partial \ell}{\partial \theta} &= \frac{2n}{\theta} + \sum_{i=1}^n \ln \left\{ 1 - \left(1 - e^{-\frac{x_i^2}{2\lambda^2}} \right)^2 \right\} - \sum_{i=1}^n \ln \left[1 - (1 - \theta) \left(1 - e^{-\frac{x_i^2}{2\lambda^2}} \right)^2 \right] \\ &- (\theta + 1) \sum_{i=1}^n \frac{1 - 2e^{-\frac{x_i^2}{2\lambda^2}} + e^{-\frac{x_i^2}{\lambda^2}}}{1 - (1 - \theta) \left(1 - e^{-\frac{x_i^2}{2\lambda^2}} \right)^2} \end{aligned} \quad (15)$$

and

$$\begin{aligned} \frac{\partial \ell}{\partial \lambda} &= -\frac{2n}{\lambda} + \frac{\sum_{i=1}^n x_i^2}{\lambda^3} - \lambda^{-3} \sum_{i=1}^n \frac{x_i^2}{1 - e^{-\frac{x_i^2}{2\lambda^2}}} + \frac{2(\theta - 1)}{\lambda^3} \sum_{i=1}^n \frac{x_i^2 \left(e^{-\frac{x_i^2}{2\lambda^2}} - e^{-\frac{x_i^2}{\lambda^2}} \right)}{1 - \left(1 - e^{-\frac{x_i^2}{2\lambda^2}} \right)^2} \\ &- \frac{2(\theta + 1)}{\lambda^3} \sum_{i=1}^n \frac{x_i^2 \left(e^{-\frac{x_i^2}{2\lambda^2}} - e^{-\frac{x_i^2}{\lambda^2}} - \theta e^{-\frac{x_i^2}{2\lambda^2}} + \theta e^{-\frac{x_i^2}{\lambda^2}} \right)}{1 - (1 - \theta) \left(1 - e^{-\frac{x_i^2}{2\lambda^2}} \right)^2} \end{aligned} \quad (16)$$

When we set equations 15 and 16 to zero, the respective solutions of θ and λ are not analytical, hence we use **optim()** function in R to resolve it.

3.2 Least Squares Estimation(LSE)

According to Swain, Venkatraman, and Wilson [39], LSEs having two parameters θ and λ , can be generated as thus;

$$\begin{aligned} E[F(x_{i:n}|\alpha, \beta, \sigma)] &= \frac{i}{n+1} \\ V[F(x_{i:n}|\alpha, \beta, \sigma)] &= \frac{i(n-i+1)}{(n+1)^2(n+2)} \end{aligned} \quad (17)$$

We obtain the estimates of $\hat{\theta}_{LSE}$, and $\hat{\lambda}_{LSE}$ having the parameter θ and λ by minimizing the function $L(\theta, \lambda)$ with respect to θ and λ

$$L(\theta, \lambda) = \operatorname{argmin} \sum_{i=1}^n \left[F(x_{i:n}|\theta, \lambda) - \frac{i}{n+1} \right]^2 \quad (18)$$

Working on the non-linear equations, we are able to obtain the estimations

$$\begin{aligned} \sum_{i=1}^n \left[F(x_{i:n}|\theta, \lambda) - \frac{i}{n+1} \right]^2 \Delta_1(x_{i:n}|\theta, \lambda) &= 0 \\ \sum_{i=1}^n \left[F(x_{i:n}|\theta, \lambda) - \frac{i}{n+1} \right]^2 \Delta_2(x_{i:n}|\theta, \lambda) &= 0 \end{aligned} \quad (19)$$

Where have the corresponding $\Delta_1(x_{i:n}|\theta, \lambda)$ and $\Delta_1(x_{i:n}|\theta, \lambda)$ as;

$$\Delta_1(x_{i:n}|\theta, \lambda) = \theta \left\{ \frac{1 - \left(1 - e^{-\frac{x^2}{2\lambda^2}}\right)^2}{1 - (1 - \theta) \left(1 - e^{-\frac{x^2}{2\lambda^2}}\right)} \right\} \frac{\left[1 - \left(1 - e^{-\frac{x^2}{2\lambda^2}}\right)^2\right] \left[1 - 2e^{-\frac{x^2}{2\lambda^2}} + e^{-\frac{x^2}{\lambda^2}}\right]}{\left\{2e^{-\frac{x^2}{2\lambda^2}} - e^{-\frac{x^2}{\lambda^2}} + \theta - 2\theta e^{-\frac{x^2}{2\lambda^2}} + \theta e^{-\frac{x^2}{\lambda^2}}\right\}^2} \quad (20)$$

$$\Delta_1(x_{i:n}|\theta, \lambda) = \frac{\left[2e^{-\frac{x^2}{2\lambda^2}} - e^{-\frac{x^2}{\lambda^2}} + \theta - 2\theta e^{-\frac{x^2}{2\lambda^2}} + 2\theta e^{-\frac{x^2}{\lambda^2}}\right] \left[\frac{2x^2}{\lambda^3} e^{-\frac{x^2}{2\lambda^2}} - \frac{2x^2}{\lambda^3} e^{-\frac{x^2}{\lambda^2}}\right]}{\left(2e^{-\frac{x^2}{2\lambda^2}} - e^{-\frac{x^2}{\lambda^2}} + \theta - 2\theta e^{-\frac{x^2}{2\lambda^2}} + \theta e^{-\frac{x^2}{\lambda^2}}\right)^2} - \frac{\left[2e^{-\frac{x^2}{2\lambda^2}} - e^{-\frac{x^2}{\lambda^2}}\right] \left[\frac{2x^2}{\lambda^3} e^{-\frac{x^2}{\lambda^2}} - \frac{2\theta x^2}{\lambda^3} e^{-\frac{x^2}{2\lambda^2}} + \frac{2\theta x^2}{\lambda^3} e^{-\frac{x^2}{\lambda^2}}\right]}{\left(2e^{-\frac{x^2}{2\lambda^2}} - e^{-\frac{x^2}{\lambda^2}} + \theta - 2\theta e^{-\frac{x^2}{2\lambda^2}} + \theta e^{-\frac{x^2}{\lambda^2}}\right)^2} \quad (21)$$

3.3 Maximum Product Space Estimator (MPSE)

Due to the Kullback Leibler measure, which approximated the general maximum product spacing method, the highest likelihood strategy has found a best fit. Let's envisage that the data are now placed in an increasing order, the peak product spacing for NER is given as

$$G_{i:m:n}(\theta, \lambda | \text{data}) = \left(\prod_{i=1}^{n+1} D_i(x_i, \theta, \lambda) \right)^{\frac{1}{n+1}} \quad (22)$$

Where $D_i(x_i, \theta, \lambda) = F(x_i; \theta, \lambda) - F(x_{i-1}; \theta, \lambda)$ $i = 1, 2, 3, \dots, n$

Following the same pace, one may decide reconstruct the function as

$$P(\theta, \lambda) = \frac{1}{n+1} \sum_{i=1}^{n+1} \ln D_i(\theta, \lambda) \quad (23)$$

To obtain the first differential equation, the function $P(\xi)$ was solved with respect to θ and λ and solving the non-linear equations at $\frac{\partial P(\xi)}{\partial \theta} = 0$ and $\frac{\partial P(\xi)}{\partial \lambda} = 0$ where $\xi = (\theta, \lambda)$

3.4 Weighted Least Square Estimation(WLSE)

Maximizing the function $W(\theta, \lambda)$ the weighted least square estimates $\hat{\theta}_{WLSE}$, and $\hat{\lambda}_{WLSE}$ NER distribution with parameter θ and λ are obtained $W(\theta, \lambda)$ with respect to θ and λ

$$W(\theta, \lambda) = \operatorname{argmin} \sum_{i=1}^n \frac{(n+1)^{\oplus}(n+2)}{i(n-i+1)} \left[F(x_{i:n}|\theta, \lambda) - \frac{i}{n+1} \right]^2 \quad (24)$$

evaluating the underlying equations yields the estimates

$$\begin{aligned} \sum_{i=1}^n \frac{(n+1)^{\oplus}(n+2)}{i(n-i+1)} \left[F(x_{i:n}|\theta, \lambda) - \frac{i}{n+1} \right]^2 \Delta_1(x_{i:n}|\theta, \lambda) &= 0 \\ \sum_{i=1}^n \frac{(n+1)^{\oplus}(n+2)}{i(n-i+1)} \left[F(x_{i:n}|\theta, \lambda) - \frac{i}{n+1} \right]^2 \Delta_2(x_{i:n}|\theta, \lambda) &= 0 \end{aligned} \quad (25)$$

where $\Delta_1(x_{i:n}|\theta, \lambda)$, $\Delta_2(x_{i:n}|\theta, \lambda)$ and $\Delta_3(x_{i:n}|\theta, \lambda)$ are stated in

3.5 Cramér-von-Mises estimation (CVME)

In order to obtain the Cramér-von-Mises estimates $\hat{\theta}_{CVME}$ and $\hat{\lambda}_{CVME}$ of NER distribution having the parameters θ and λ we will have to minimize the function $C(\theta, \lambda)$ with respect to θ and λ

$$C(\theta, \lambda) = \operatorname{argmin} \left\{ \frac{1}{12} + \sum_{i=1}^n \left[F(x_{i:n}|\theta, \lambda) - \frac{2i-1}{2n} \right]^2 \right\} \quad (26)$$

evaluating the underlying equations yields the estimates

$$\begin{aligned} \sum_{i=1}^n \left(F(x_{i:n}|\theta, \lambda) - \frac{2i-1}{2n} \right)^2 \Delta_1(x_{i:n}|\theta, \lambda) &= 0 \\ \sum_{i=1}^n \left(F(x_{i:n}|\theta, \lambda) - \frac{2i-1}{2n} \right)^2 \Delta_2(x_{i:n}|\theta, \lambda) &= 0 \end{aligned} \quad (27)$$

where $\Delta_1(x_{i:n}|\theta, \lambda)$, $\Delta_2(x_{i:n}|\theta, \lambda)$ and $\Delta_3(x_{i:n}|\theta, \lambda)$ are stated in

3.6 Anderson-Darling estimation (ADE)

In order to obtain the Anderson-Darling estimates $\hat{\theta}_{ADE}$ and $\hat{\lambda}_{ADE}$ of NER distribution having the parameters θ and λ we will have to minimize the function $C(\theta, \lambda)$ with respect to θ and λ

$$A(\theta, \lambda) = \operatorname{argmin} \sum_{i=1}^n (2i-1) \{ \ln F(x_{i:n}|\theta, \lambda) - [1 - F(x_{i:n}|\theta, \lambda)] \} \quad (28)$$

evaluating the underlying equations yields the estimates

$$\begin{aligned} \sum_{i=1}^n \left[\frac{\Delta_1(x_{i:n}|\theta, \lambda)}{F(x_{i:n}|\theta, \lambda)} - \frac{\Delta_1(x_{n+1=i:n}|\theta, \lambda)}{1 - F(x_{n+1=i:n}|\theta, \lambda)} \right] &= 0 \\ \sum_{i=1}^n \left[\frac{\Delta_2(x_{i:n}|\theta, \lambda)}{F(x_{i:n}|\theta, \lambda)} - \frac{\Delta_2(x_{n+1=i:n}|\theta, \lambda)}{1 - F(x_{n+1=i:n}|\theta, \lambda)} \right] &= 0 \end{aligned} \quad (29)$$

where $\Delta_1(x_{i:n}|\theta, \lambda)$, $\Delta_2(x_{i:n}|\theta, \lambda)$ and $\Delta_3(x_{i:n}|\theta, \lambda)$ are stated in

3.7 Right-Tailed Anderson-Darling estimation (RTADE)

In order to obtain the Right-Tailed Anderson-Darling estimates $\hat{\theta}_{RTADE}$ and $\hat{\lambda}_{RTADE}$ of NER distribution having the parameters θ and λ we will have to minimize the function $C(\theta, \lambda)$ with respect to θ and λ

$$A(\theta, \lambda) = \operatorname{argmin} \left\{ \frac{n}{2} - 2 \sum_{i=1}^n F(x_{i:n}|\theta, \lambda) - \frac{1}{2} \sum_{i=1}^n (2i-1) \ln [1 - F(x_{n+1=i:n}|\theta, \lambda)] \right\} \quad (30)$$

evaluating the underlying equations yields the estimates

$$\begin{aligned} -2 \sum_{i=1}^n \frac{\Delta_1(x_{i:n}|\theta, \lambda)}{F(x_{i:n}|\theta, \lambda)} + \frac{1}{n} \sum_{i=1}^n (2i-1) \left[\frac{\Delta_1(x_{n+1=i:n}|\theta, \lambda)}{1 - F(x_{n+1=i:n}|\theta, \lambda)} \right] &= 0 \\ -2 \sum_{i=1}^n \frac{\Delta_2(x_{i:n}|\theta, \lambda)}{F(x_{i:n}|\theta, \lambda)} + \frac{1}{n} \sum_{i=1}^n (2i-1) \left[\frac{\Delta_2(x_{n+1=i:n}|\theta, \lambda)}{1 - F(x_{n+1=i:n}|\theta, \lambda)} \right] &= 0 \end{aligned} \quad (31)$$

where $\Delta_1(x_{i:n}|\theta, \lambda)$, $\Delta_2(x_{i:n}|\theta, \lambda)$ and $\Delta_3(x_{i:n}|\theta, \lambda)$ are stated in.

The evolutionary development were further evaluated in the software, R, see Team [40].

3.8 Bayesian Estimation

In this section, we obtain Bayesian estimates that take parameter uncertainties into account and deal with the parameters as random variables. The joint prior distribution is used to define the knowledge of the parameter uncertainties before the gathering of failure data. Because it allows for the addition of prior information in the analysis, the Bayesian approach is very helpful in reliability analysis. This is significant because the lack of readily available data is one of the major hassles with reliability research. The unknown parameter θ , and λ is estimated using the Bayesian estimation (BE) technique under the assumption that its prior distribution is uninformative. Also, applying gamma prior for the variables θ , and λ with p.d.fs in the parameter prior distribution of NER.

$$\begin{aligned}\pi_1(\theta) &\propto \theta^{k_1-1} e^{-t_1\theta} \\ \pi(\lambda) &\propto \lambda^{k_2-1} e^{-t_1\lambda}\end{aligned}\quad (32)$$

Where the hyper parameter $k_s, t_s, s = 1, 2$ are selected to reject the prior knowledge about the unknown parameter. The joint prior for $\psi = (\theta, \lambda)$ is given by

$$\begin{aligned}\pi(\psi) &= \pi_1(\theta)\pi_2(\lambda) \\ \pi(\psi) &\propto \theta^{k_1-1} \lambda^{k_2-1} e^{\{-t_1\theta - t_2\lambda\}}\end{aligned}\quad (33)$$

The corresponding posterior distribution density given the observed data $x = (x_1, x_2, \dots, x_n)$ is given by

$$\pi(\psi | \mathbf{x}) = \frac{\pi(\psi)\ell(\psi)}{\int_{\psi} \pi(\psi)\ell(\psi)d\psi}$$

Consequently, the posterior density function is given by

$$\begin{aligned}\pi(\psi | \mathbf{x}) &\propto \theta^{k_1-1} \lambda^{k_2-1} e^{\{-t_1\theta - t_2\lambda\}} \frac{2^n \theta^{2n}}{\lambda^{2n}} e^{-\frac{\sum_{i=1}^n x_i^2}{2\lambda^2}} \prod_{i=1}^n \left(1 - e^{-\frac{x_i^2}{2\lambda^2}}\right) \\ &\times \left\{1 - \left(1 - e^{-\frac{x_i^2}{2\lambda^2}}\right)^2\right\}^{\theta-1} \left[1 - (1 - \theta) \left(1 - e^{-\frac{x_i^2}{2\lambda^2}}\right)^2\right]^{-(\theta+1)}\end{aligned}\quad (34)$$

Given any function, such as $l(\psi)$ under the squared error loss (SEL) function, the Bayes estimator is given as

$$\hat{\psi}_{BE_{SEL}} = E[l(\psi) | \mathbf{x}] = \int_{\psi} l(\psi) \pi(\psi | x) d\psi \quad (35)$$

The SEL being a symmetrical loss function regards overestimation and underestimation equally. In real-life situations, both overestimation and underestimation can have serious implications. The linear exponential loss function (LINEX) can be used in certain instances as an alternative to the SEL function given by

$$(l(\psi), \hat{l}(\psi)) = e^{\{\hat{l}(\psi) - l(\psi)\}} - \tau(\hat{l}(\psi) - l(\psi)) - 1$$

Where $\tau \neq 0$ is a shape parameter. Here, $\tau > 1$ insinuates that an overestimation is more serious than an underestimation and vice-versa for $\tau < 0$. Further, as τ approaches zero it replicates the SE loss function. For more details in this regard one should refer to Varian [43] and Doostparast, Akbari, and Balakrishna [12]. The BE of $l(\psi)$ under this loss function is given by

$$\psi_{BE_{LINEX}} = E[e^{\{-\tau(\psi)\}} | \mathbf{x}] = -\frac{1}{\tau} \log \left[\int_{\psi} e^{\{-\tau(\psi)\}} \pi(\psi | x) d\psi \right] \quad (36)$$

Likewise, we consider the general entropy loss (GEL) suggested by Calabria and Pulcini [9] defined as

$$(l(\psi), \hat{l}(\psi)) = \left(\frac{\hat{l}(\psi)}{l(\psi)} \right)^{\nu} - \nu \log \left(\frac{\hat{l}(\psi)}{l(\psi)} \right) - 1$$

Where $\nu \neq 0$ denotes a divergence from symmetry. It views overestimation as more significant than underestimation when $\nu > 0$ and vice-versa when $\nu < 0$. The Bayes estimator of $l(\psi)$ under the GE loss function is as follows

$$\psi_{BE_{GEL}} = [E((l(\psi))^{-\nu} | x)]^{-\frac{1}{\nu}} = \left[\int_{\psi} (l(\psi))^{-\nu} \pi(\psi | x) d\psi \right]^{-\frac{1}{\nu}} \quad (37)$$

Where there is no analytical solution to the computation of equation 35, 36 and 37, the Markov chain Monte Carlo (MCMC) approach to generate posterior samples and arrive at suitable BE_s is then used. It is possible to properly quantify the posterior uncertainty with respect to the parameter ψ using a kernel estimate of the posterior distribution and the MCMC samples.

Lastly, part of the initial samples can be eliminated (burn-in) from the random samples of size M derived from the posterior density, and the remaining samples can then be used to calculate Bayes estimates. Using MCMC under the SEL, LINEX, and GEL functions, the BE_s of $\psi^i = (\theta)^i, (\lambda)^i$ can be calculated as

$$\hat{\psi}_{BE_{SEL}} = \frac{1}{M - l_B} \sum_{i=l_B}^M \psi^{(i)} \quad (38)$$

$$\hat{\psi}_{BE_{LINEX}} = -\frac{1}{\tau} \log \left[\frac{1}{M - l_B} \sum_{i=l_B}^M e^{\{-\tau \psi^{(i)}\}} \right] \quad (39)$$

$$\hat{\psi}_{BE_{GEL}} = \left[\frac{1}{M - l_B} \sum_{i=l_B}^M \left(\psi^{(i)} \right)^{-\nu} \right]^{\frac{-1}{\nu}} \quad (40)$$

where l_B represents the number of burn-in samples.

3.9 Credible Intervals for Bayesian Estimates

A $100(1 - \gamma)\%$ credible intervals for the parameters $\psi = (\theta, \lambda)$ under the loss functions discussed are

$$\hat{\psi}_{BE_{SEL}} \pm Z_{\frac{\gamma}{2}} \sqrt{var \hat{\psi}_{BE_{SEL}}}; \quad \hat{\psi}_{BE_{LINEX}} \pm Z_{\frac{\gamma}{2}} \sqrt{var \hat{\psi}_{BE_{LINEX}}}; \quad \hat{\psi}_{BE_{GEL}} \pm Z_{\frac{\gamma}{2}} \sqrt{var \hat{\psi}_{BE_{GEL}}} \quad (41)$$

where $Z_{\frac{\gamma}{2}}$ is the percentile standard normal distribution with right-tailed probability

4 Simulation

In this section, we are to introduce the data simulation for the NER distribution in order to compare the capabilities of the Bayesian and Non-Bayesian estimation methods which were studied in the previous section. Some random data were generated from the NER distribution by choosing the initial parameter values as;

- case I: $\theta = 0.5$ and $\lambda = 0.75$
- case II: $\theta = 0.75$ and $\lambda = 1.75$
- case III: $\theta = 0.75$ and $\lambda = 1.25$

and corresponding sample sizes $n = 25, 50, 75, 100$. For each of the estimates $\hat{\psi} = (\hat{\theta}, \hat{\lambda})$. we are going to compute the Bias and Root Mean Squared Error (RMSE) respectively as

$$Bias(\psi) = \frac{1}{N} \sum_{i=1}^N (\hat{\psi}_1 - \psi) \quad (42)$$

$$RMSE = \sqrt{\frac{1}{N} \sum_{i=1}^N (\hat{\psi}_1 - \psi)^2}$$

In the Non-Bayesian approach, we utilized the Newton-Raphson algorithm to compute the desired estimates. In contrast, for the Bayesian approach, posterior estimates were obtained using Markov Chain Monte Carlo (MCMC) methods, specifically employing the Metropolis-Hastings algorithm under an informative prior.

Table 1: Simulation results using $\theta = 0.5, \lambda = 0.75$

		$n = 25$		$n = 50$		$n = 75$		$n = 100$	
		Bias	RMSE	Bias	RMSE	Bias	RMSE	Bias	RMSE
MLE	θ	0.1193	0.0164	0.1215	0.0159	0.1213	0.0154	0.1217	0.0153
	λ	0.7456	0.5576	0.7446	0.5552	0.7424	0.5517	0.7418	0.5507
LSE	θ	0.0671	0.0410	0.0522	0.0355	0.0488	0.0330	0.0434	0.0324
	λ	0.2123	0.3317	0.1762	0.3108	0.1654	0.2873	0.1509	0.2834
WLSE	θ	0.0110	0.0262	0.0081	0.0226	0.0100	0.0204	0.0017	0.0205
	λ	0.0699	0.2082	0.0542	0.1818	0.0553	0.1647	0.0297	0.1590
MPSE	θ	0.0051	0.0288	0.0055	0.0262	0.0017	0.0222	0.0017	0.0223
	λ	0.0593	0.2300	0.0518	0.2107	0.0361	0.1752	0.0245	0.1742
CVME	θ	0.0330	0.0274	0.0141	0.0245	0.0119	0.0210	0.0142	0.0212
	λ	0.0441	0.2092	0.0022	0.1951	0.0037	0.1601	0.0116	0.1627
ADE	θ	0.0061	0.0325	0.0040	0.0265	0.0006	0.0230	0.0056	0.0226
	λ	0.0328	0.2591	0.0261	0.2108	0.0315	0.1878	0.0144	0.1785
RTADE	θ	0.1117	0.0141	0.1120	0.0133	0.1129	0.0132	0.1131	0.0132
	λ	0.7313	0.5411	0.7523	0.5677	0.7591	0.5771	0.7626	0.5821
BE_{SEL}	θ	0.1123	0.0142	0.1123	0.0134	0.1131	0.0133	0.1133	0.0132
	λ	0.7389	0.5524	0.7565	0.5742	0.7620	0.5816	0.7648	0.5855
BE_{Linex1}	θ	0.1112	0.0139	0.1117	0.0132	0.1127	0.0132	0.1130	0.0131
	λ	0.7238	0.5300	0.7480	0.5613	0.7561	0.5726	0.7603	0.5786
BE_{Linex2}	θ	0.1109	0.0139	0.1116	0.0132	0.1126	0.0132	0.1129	0.0131
	λ	0.7262	0.5336	0.7494	0.5634	0.7571	0.5741	0.7611	0.5798
BE_{GEL1}	θ	0.1091	0.0135	0.1106	0.0130	0.1120	0.0130	0.1124	0.0130
	λ	0.7160	0.5189	0.7438	0.5550	0.7532	0.5682	0.7581	0.5753
BE_{GEL2}	θ	0.0300	0.0347	0.0219	0.0291	0.0263	0.0274	0.0245	0.0274
	λ	0.1237	0.2954	0.0904	0.2404	0.1023	0.2337	0.0964	0.2332

Table 2: Simulation results using $\theta = 0.75, \lambda = 1.75$

		$n = 25$		$n = 50$		$n = 75$		$n = 100$	
		Bias	RMSE	Bias	RMSE	Bias	RMSE	Bias	RMSE
MLE	θ	0.0354	0.0025	0.0357	0.0019	0.0355	0.0017	0.0348	0.0015
	λ	0.2495	0.0636	0.2476	0.0621	0.2463	0.0612	0.2457	0.0608
LSE	θ	0.2196	1.9407	0.0760	0.1523	0.0538	0.0413	0.0455	0.0346
	λ	6.9081	5445.8514	0.7605	130.4801	0.3020	1.1584	0.2538	0.9659
WLSE	θ	0.5527	3.5883	0.2363	0.8174	0.1496	0.3298	0.0979	0.0829
	λ	13.5874	3906.3340	3.4240	534.9704	1.6157	253.4976	0.6395	8.5511
MPSE	θ	0.5638	4.2881	0.2220	0.7587	0.1333	0.2611	0.0852	0.0612
	λ	15.5488	6661.6155	3.2798	898.7992	1.2862	134.5164	0.5085	2.8090
CVME	θ	0.9719	7.6396	0.3548	1.4612	0.1940	0.3659	0.1294	0.1364
	λ	27.9427	11432.7085	5.9845	1380.8134	1.9014	208.3366	0.9484	35.1685
ADE	θ	0.5601	3.9043	0.2034	0.4649	0.1272	0.0889	0.0941	0.0649
	λ	14.6323	7010.2827	2.2162	360.7509	0.7494	3.2980	0.5549	3.4225
RTADE	θ	0.5029	4.0466	0.1820	0.6007	0.1054	0.1046	0.0765	0.0584
	λ	15.1728	9500.9365	2.4776	704.8319	0.7184	14.2632	0.4569	2.2563
BE _{SEL}	θ	0.7651	0.6060	0.7664	0.5975	0.7691	0.5981	0.7699	0.5977
	λ	0.0502	0.0130	0.0626	0.0084	0.0658	0.0069	0.0679	0.0064
BE _{Linex1}	θ	0.7672	0.6094	0.7675	0.5992	0.7698	0.5993	0.7704	0.5986
	λ	0.0561	0.0138	0.0659	0.0088	0.0681	0.0072	0.0696	0.0067
BE _{Linex2}	θ	0.7630	0.6027	0.7653	0.5958	0.7684	0.5970	0.7693	0.5969
	λ	0.0443	0.0123	0.0593	0.0079	0.0636	0.0066	0.0661	0.0062
BE _{GEL1}	θ	0.7635	0.6035	0.7655	0.5962	0.7685	0.5972	0.7694	0.5970
	λ	0.0456	0.0126	0.0601	0.0081	0.0641	0.0066	0.0666	0.0062
BE _{GEL2}	θ	0.7602	0.5983	0.7638	0.5935	0.7674	0.5955	0.7686	0.5957
	λ	0.0366	0.0118	0.0551	0.0075	0.0607	0.0062	0.0639	0.0059

Table 3: Simulation results using $\theta = 0.75, \lambda = 1.25$

		$n = 25$		$n = 50$		$n = 75$		$n = 100$	
		Bias	RMSE	Bias	RMSE	Bias	RMSE	Bias	RMSE
MLE	θ	0.0544	0.0058	0.0515	0.0042	0.0509	0.0035	0.0536	0.0036
	λ	0.2472	0.0625	0.2477	0.0621	0.2469	0.0615	0.2461	0.0609
LSE	θ	0.4000	7.9156	0.1041	0.2024	0.0886	0.0987	0.0548	0.0687
	λ	13.3239	18432.9114	0.4879	12.1045	0.3243	1.1968	0.2099	0.7129
WLSE	θ	0.8371	8.9584	0.3306	1.5739	0.2086	0.4163	0.1458	0.2137
	λ	14.5385	4963.4989	3.0989	613.1665	1.1124	58.5444	0.6703	10.6370
MPSE	θ	0.8145	9.1095	0.2977	1.2402	0.1870	0.3298	0.1258	0.1398
	λ	14.8396	5697.0382	2.5110	409.1226	0.9302	49.0345	0.5077	2.3837
CVME	θ	1.3939	15.3278	0.4841	2.3676	0.2818	0.5899	0.1952	0.3133
	λ	25.3243	9133.8600	4.6457	874.1430	1.5470	82.4473	0.9425	23.6100
ADE	θ	0.7987	9.8472	0.2787	0.6476	0.1980	0.2396	0.1355	0.1345
	λ	15.9269	8984.6902	1.5571	91.2785	0.8221	7.5643	0.5253	1.9631
RTADE	θ	0.7612	8.8600	0.2338	0.6193	0.1847	0.4635	0.1018	0.1192
	λ	15.2619	7526.1640	1.4013	89.9658	1.1216	137.6334	0.4105	1.7639
BE_{SEL}	θ	0.4379	0.2123	0.4388	0.2025	0.4412	0.2012	0.4419	0.2002
	λ	0.0005	0.0119	0.0102	0.0054	0.0131	0.0032	0.0145	0.0024
BE_{Linex1}	θ	0.4398	0.2141	0.4397	0.2034	0.4419	0.2018	0.4424	0.2007
	λ	0.0061	0.0121	0.0133	0.0055	0.0152	0.0033	0.0161	0.0025
BE_{Linex2}	θ	0.4361	0.2105	0.4378	0.2017	0.4406	0.2006	0.4414	0.1998
	λ	0.0050	0.0118	0.0072	0.0053	0.0110	0.0031	0.0129	0.0024
BE_{GEL1}	θ	0.4364	0.2109	0.4380	0.2018	0.4407	0.2007	0.4415	0.1999
	λ	0.0039	0.0119	0.0078	0.0053	0.0115	0.0032	0.0132	0.0024
BE_{GEL2}	θ	0.4333	0.2081	0.4364	0.2004	0.4396	0.1998	0.4407	0.1992
	λ	0.0127	0.0119	0.0030	0.0053	0.0081	0.0031	0.0107	0.0023

The following deductions can be made from the simulation studies;

1. For sample size $n = 25$, the RMSE of λ from all the non-bayesian methods except MLE are unusually high.
2. As the sample increases, the RMSE for θ using MLE has the minimum value, while the BE_{GEL2} for λ has the minimum value.
3. Obviously, for all the methods, as the sample size increases, the RMSE decreases showing consistency.
4. Again, the Bias remain positive for all the methods as the sample size increases.

5 Application

First, we consider the mortality rate of COVID-19 patients in Holland and analyze, see Almongy et al. [5], Zhou et al. [44].

7.4590	3.7490	3.4700	5.3280	1.4285	1.1270	6.1350
5.1445	5.4160	1.7305	1.8235	2.9640	6.6055	3.9840
3.7920	2.6535	2.5240	2.7155	2.7775	3.0135	2.0485
1.8055	2.4800	2.2310	1.9415	0.9870		

Table 4: MLEs for some fitted models to the data on mortality rates of COVID 19 patients and the AIC, W^* and A^* value

Model	a	b	l	k	t	W^*	A^*	AIC	CAIC	BIC	HQIC
NER	—	—	2.165	—	1.491	0.05	0.345	99.132	99.632	101.724	99.903
GIE	5.398	—	5.985	—	—	0.020	0.173	102.744	103.244	105.335	103.514
Weibull	2.068	3.788	—	—	—	0.072	0.434	104.428	104.244	107.002	105.181
EW	8.963	—	0.922	0.830	—	0.021	0.165	104.289	105.332	108.176	105.445
LN	1.089	0.528	—	—	—	0.020	0.159	102.760	103.260	103.530	103.530

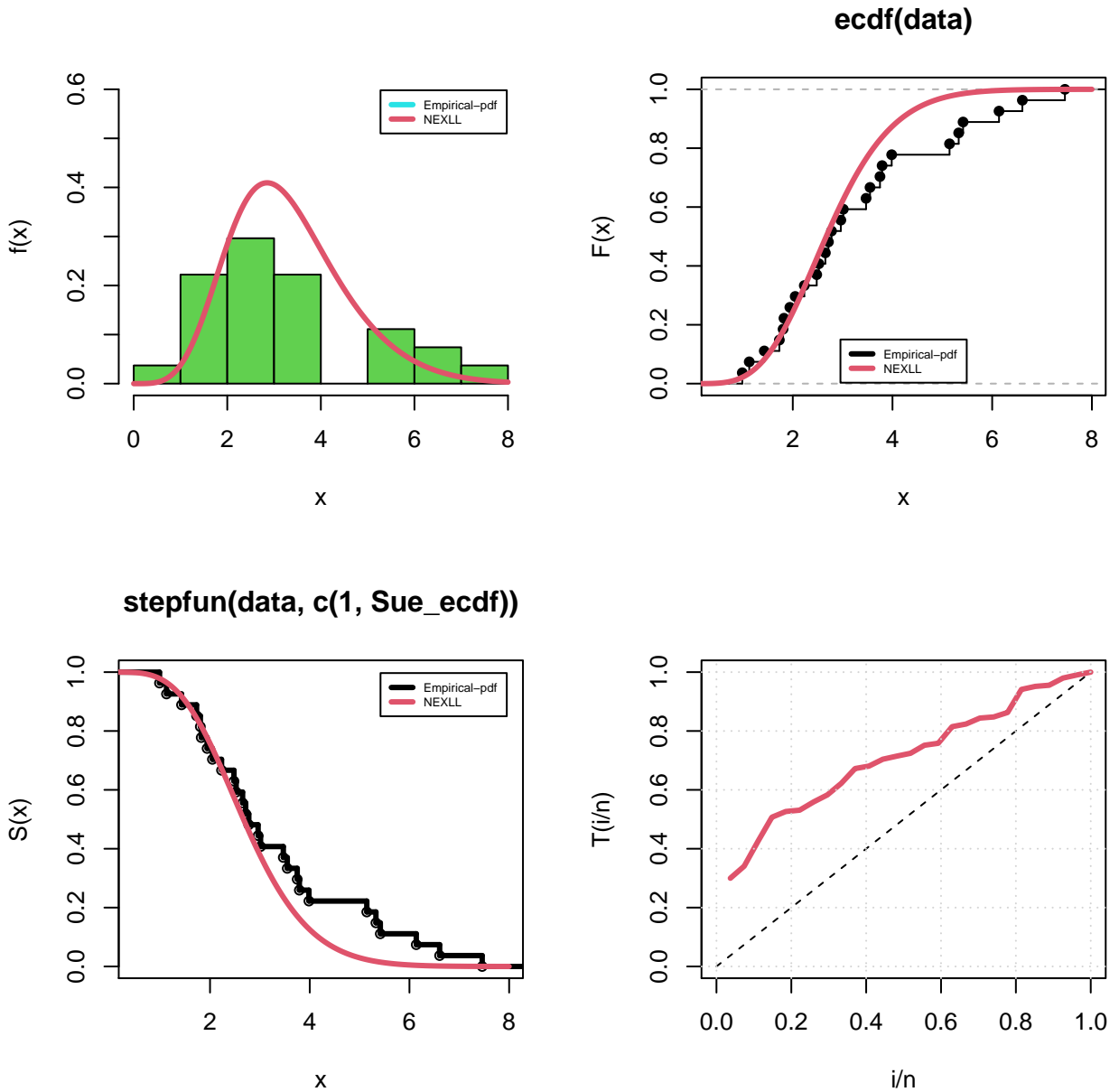


Figure 11: Histogram, c.d.f, Survival, TTT plots (θ, λ)

The second application is on the relief times (in minutes) of patients who analgesic were administered to, see Oguntunde, Adejumo, and Owoloko [29], Shanker et al. [37] observations as follows :

1.1	1.4	1.3	1.7	1.9	1.8	1.6	2.2	1.7	2.7
4.1	1.8	1.5	1.2	1.4	3	1.7	2.3	1.6	2

Table 5: MLEs for some fitted models to data

Model	a	b	l	k	t	AIC	CAIC	BIC	HQIC	W	A
NER	—	—	1.257	—	1.586	33.364	34.069	35.355	33.752	0.124	0.739
GIE	20.770	—	6.171	—	—	38.209	38.915	40.200	38.597	0.080	0.475
Weibull	2.791	2.118	—	—	—	45.177	45.883	47.169	45.566	0.186	1.096
EW	$3.4E^{03}$	—	$1.8e^{-02}$	—	—	37.087	38.587	40.074	37.670	0.033	0.189
LN	0.601	0.388	—	—	—	39.311	40.017	41.303	39.700	0.072	0.425

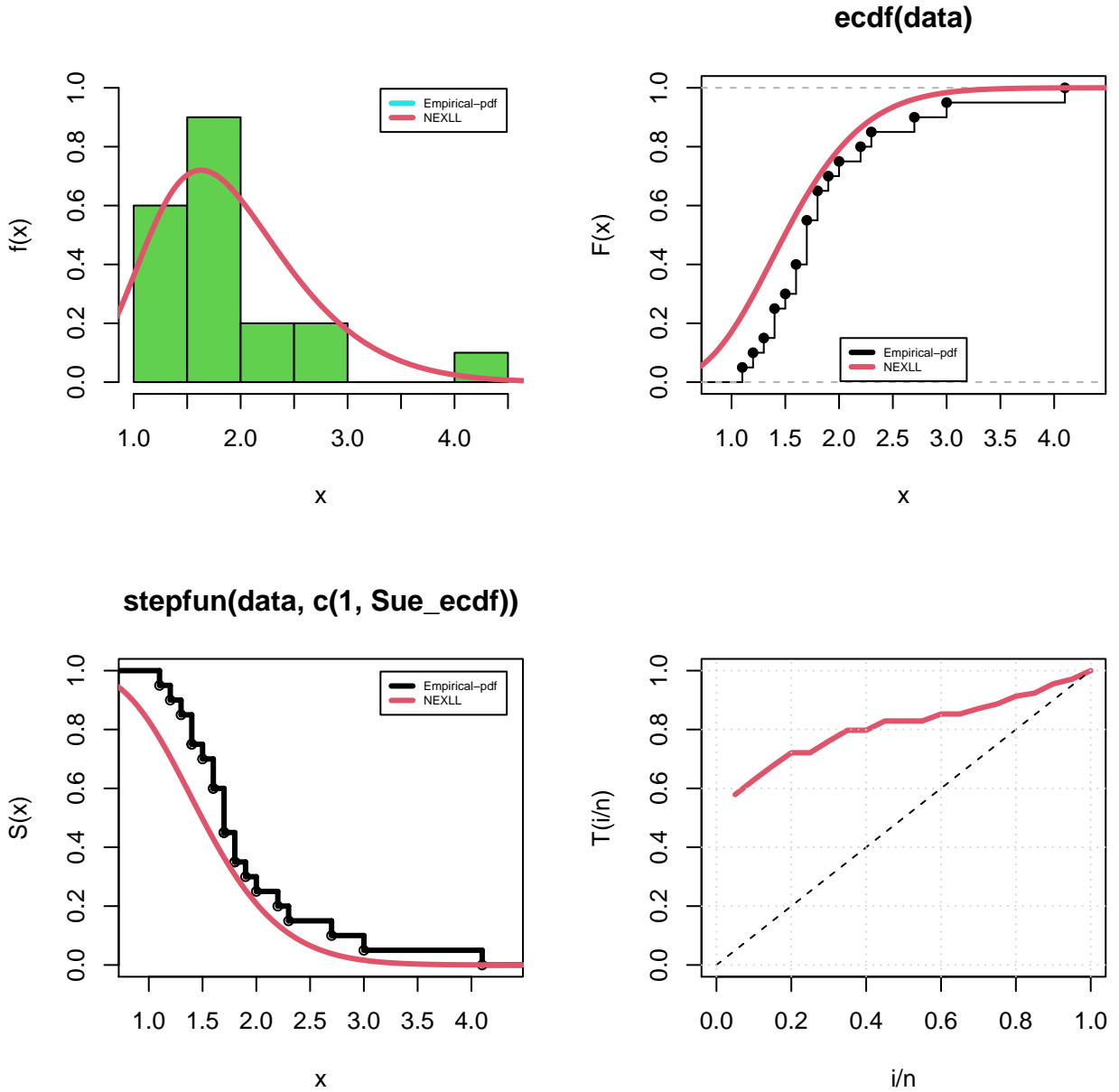


Figure 12: Histogram, c.d.f, Survival, TTT plots (θ, λ)

For the real data analysis using data set mortality rates of COVID 19 patients and the relief times (in minutes) of patients who analgesic were administered to, the Akaike Information Criterion (AIC), Corrected AIC (CAIC), Bayesian Information Criterion (BIC) and Hannan-Quinn Information Criterion (HQIC) of the NER distribution have the least values using both data sets as compared to GIE, Weibull, EW, LN. Therefore, it is safe to say that the NER distribution performed better.

Figures 11, 12 Histogram, c.d.f, Survival and TTT plots of the NER distribution for COVID 19 and pain relief data.

6 Conclusion

A distribution named NER, gotten from the NEX family was created in this paper. The p.d.f assumed a reverse bath-tub shape and is noticed to be right-tailed. Several mathematical properties such as moment, quantile function (which has a closed form), the shape the distribution takes, shanon entropy, and also its mean, the 3-dimensional plots of the kurtosis, skewness, mean and variance, which further displays the ability of the parameters to act as both shape and scale. Bayesian point estimate were conducted for the distribution, which includes the squared error, LINEX, where we have LINEX 1 and LINEX 2 and also GEL1 and GEL2 because of their symmetric nature, and the generalized entropy loss function. The writers also used the Markov chain Monte Carlo (MCMC) approach to generate posterior samples and arrived at suitable BEs. The writers also discussed the maximum likelihood function. Using AIC, BIC, CAIC, HQIC statistic, the test for the goodness of fit was conducted. From two data sets, it shows that the NER has a better performance than few of its competitors having the least values from these estimations. The parametric plots containing the histogram, c.d.f, survival and TTT plots gotten from both data sets are displayed which show good fits to the two data sets.

Conflict of Interest

The authors have no conflict of any form of interest.

References

- [1] Musa Abuh, Sidney I Onyeagu, and Okechukwu Obulezi. “Comparative Study Based on Simulation of Some Methods of Classical Estimation of the Parameters of Exponentiated Lindley–Logarithmic Distribution”. In: *Asian Journal of Probability and Statistics* 22.4 (2023), pp. 14–30.
- [2] Afaq Ahmad, SP Ahmad, and A Ahmed. “Transmuted inverse Rayleigh distribution: A generalization of the inverse Rayleigh distribution”. In: *Mathematical Theory and Modeling* 4.7 (2014), pp. 90–98.
- [3] Z Ahmed, Zohdy M Nofal, N Ebraheim Abd El Hadi, et al. “Exponentiated transmuted generalized Raleigh distribution: A new four parameter Rayleigh distribution”. In: *Pakistan journal of statistics and operation research* (2015), pp. 115–134.
- [4] Osama Abdulaziz Alamri et al. “Statistical modelling for the Covid-19 mortality rate in the Kingdom of Saudi Arabia”. In: *Alexandria Engineering Journal* 68 (2023), pp. 517–526.
- [5] Hisham M Almongy et al. “A new extended Rayleigh distribution with applications of COVID-19 data”. In: *Results in Physics* 23 (2021), p. 104012.
- [6] Kahkashan Ateeq, Tahira Bano Qasim, and Ayesha Rehman Alvi. “An extension of Rayleigh distribution and applications”. In: *Cogent Mathematics & Statistics* 6.1 (2019), p. 1622191.
- [7] Majdah Mohammed Badr, Amal T Badawi, Alya S Alzubidi, et al. “A New Extension of the Exponentiated Weibull Model Mathematical Properties and Modelling”. In: *Journal of Function Spaces* 2022 (2022).
- [8] AA Bhat and S Parvaiz Ahmad. “A NEW GENERALIZATION OF RAYLEIGH DISTRIBUTION: PROPERTIES AND APPLICATIONS.” In: *Pakistan journal of statistics* 36.3 (2020).
- [9] R Calabria and G Pulcini. “Point estimation under asymmetric loss functions for left-truncated exponential samples”. In: *Communications in Statistics-Theory and Methods* 25.3 (1996), pp. 585–600.
- [10] Eberechukwu Q Chinedu et al. “New lifetime distribution with applications to single acceptance sampling plan and scenarios of increasing hazard rates”. In: *Symmetry* 15.10 (2023), p. 1881.
- [11] Prince O Chukwuma et al. “A new reduced quantile function for generating families of distributions”. In: *Annals of Mathematics and Physics* 7.1 (2024), pp. 001–015.

- [12] Mahdi Doostparast, Mohammad Ghasem Akbari, and N Balakrishna. “Bayesian analysis for the two-parameter Pareto distribution based on record values and times”. In: *Journal of Statistical Computation and Simulation* 81.11 (2011), pp. 1393–1403.
- [13] Divine-Favour N Ekemezie and Okechukwu J Obulezi. “The Fav-Jerry Distribution: Another Member in the Lindley Class with Applications”. In: *Earthline Journal of Mathematical Sciences* 14.4 (2024), pp. 793–816.
- [14] Harrison O Etaga et al. “A New Modification of Rani Distribution with More Flexibility in Application”. In: *Sch J Phys Math Stat* 7 (2023), pp. 160–176.
- [15] Harrison O Etaga et al. “A new modification of Shanker distribution with applications to increasing failure rate data”. In: *Earthline Journal of Mathematical Sciences* 13.2 (2023), pp. 509–526.
- [16] Harrison O Etaga et al. “An improved XShanker distribution with applications to rainfall and vinyl chloride data”. In: *Sch J Eng Tech* 9 (2023), pp. 212–224.
- [17] Harrison O Etaga et al. “Estimation of the Xrama distribution parameter under complete and progressive type-II censored schemes”. In: *Sch J Phys Math Stat* 10 (2023), pp. 203–219.
- [18] Harrison O Etaga et al. “The Double XLindley Distribution: Properties and Applications”. In: *Sch J Phys Math Stat* 10 (2023), pp. 192–202.
- [19] Mutua Kilai et al. “A new versatile modification of the Rayleigh distribution for modeling COVID-19 mortality rates”. In: *Results in Physics* 35 (2022), p. 105260.
- [20] Raj Kamal Maurya et al. “On a generalized Lomax distribution”. In: *International Journal of System Assurance Engineering and Management* 10 (2019), pp. 1091–1104.
- [21] Faton Merovci and Ibrahim Elbatal. “Weibull Rayleigh distribution: Theory and applications”. In: *Appl. Math. Inf. Sci* 9.5 (2015), pp. 1–11.
- [22] Abuh Musa, Sidney I Onyeagu, and Okechukwu J Obulezi. “Exponentiated Power Lindley-Logarithmic distribution and its applications”. In: *Asian Research Journal of Mathematics* 19.8 (2023), pp. 47–60.
- [23] Bright C Nwankwo et al. “Group acceptance sampling plans for type-I heavy-tailed exponential distribution based on truncated life tests”. In: *AIP Advances* 14.3 (2024).
- [24] Bright Chimezie Nwankwo et al. “A new distribution for modeling both blood cancer data and median effective dose (ED50) of Artemether-Lumefantrine against *P. falciparum*”. In: *Earthline Journal of Mathematical Sciences* 14.1 (2024), pp. 41–62.
- [25] Mmesoma Peace Nwankwo, Bright Chimezie Nwankwo, and Okechukwu Jeremiah Obulezi. “The Exponentiated Power Akash Distribution: Properties, Regression, and Applications to Infant Mortality Rate and COVID-19 Patients’ Life Cycle”. In: *Annals of Biostatistics and Biometric Applications* 5.4 (2023), pp. 1–12.
- [26] Okechukwu J Obulezi et al. “Modeling Mortality Rate of COVID-19 Patients in the United Kingdom, Canada, and the Survival Rate of COVID-19 Patients in Spain”. In: *Journal of Xidian University* 17.11 (2023), pp. 520–538.
- [27] Okechukwu J Obulezi et al. “The Exponentiated Power Chris-Jerry Distribution: Properties, Regression, Simulation and Applications to Infant Mortality Rate and Lifetime of COVID-19 Patients”. In: *TWIST* 18.4 (2023), pp. 328–337.
- [28] Okechukwu J Obulezi et al. “The Kumaraswamy Chris-Jerry distribution and its applications”. In: *Journal of Xidian University* 17.6 (2023), pp. 575–591.
- [29] PE Oguntunde, Adebawale Olusola Adejumo, and EA Owoloko. “Application of Kumaraswamy inverse exponential distribution to real lifetime data”. In: *International Journal of Applied Mathematics and Statistics* 56.5 (2017), pp. 34–47.
- [30] FC Oha et al. “Power XShanker Distribution: Properties, Estimation, and Applications”. In: *Eng OA* 2.1 (2024), pp. 01–20.
- [31] Henry Chukwuemeka Onuoha et al. “The Weibull distribution with estimable shift parameter”. In: *Earthline Journal of Mathematical Sciences* 13.1 (2023), pp. 183–208.
- [32] Chrisogonus K Onyekwere et al. “Modification of Shanker distribution using quadratic rank transmutation map”. In: *Journal of Xidian University* 16.8 (2022), pp. 179–198.

- [33] Dorathy O Oramulu et al. “A new member in the Lindley class of distributions with flexible applications”. In: *Sch J Phys Math Stat* 7 (2023), pp. 148–159.
- [34] Dorathy O Oramulu et al. “Simulation study of the Bayesian and non-Bayesian estimation of a new lifetime distribution parameters with increasing hazard rate”. In: *Asian Research Journal of Mathematics* 19.9 (2023), pp. 183–211.
- [35] Gadde Srinivasa Rao and Sauda Mbawambo. “Exponentiated inverse Rayleigh distribution and an application to coating weights of iron sheets data”. In: *Journal of probability and statistics* 2019.1 (2019), p. 7519429.
- [36] G Archdall Reid. “The problem of the random walk”. In: *Nature* 72.1866 (1905), pp. 318–319.
- [37] Rama Shanker et al. “On modeling of lifetime data using two-parameter gamma and Weibull distributions”. In: *Biometrics & Biostatistics International journal* 4.5 (2016), pp. 1–6.
- [38] A Soliman, Essam A Amin, and Alaa A Abd-El Aziz. “Estimation and prediction from inverse Rayleigh distribution based on lower record values”. In: *Applied Mathematical Sciences* 4.62 (2010), pp. 3057–3066.
- [39] James J Swain, Sekhar Venkatraman, and James R Wilson. “Least-squares estimation of distribution functions in Johnson’s translation system”. In: *Journal of Statistical Computation and Simulation* 29.4 (1988), pp. 271–297.
- [40] R Core Team. “R language and environment for statistical computing, R Foundation for Statistical”. In: *Computing* (2020).
- [41] Getachew Tekle, Rasool Roozegar, and Hamid Bidram. “A new alpha power type-1 family of distributions and modelling the overdispersed count outcome”. In: *Journal of Statistical Modelling: Theory and Applications* 3.1 (2023), pp. 83–101.
- [42] Ahlam H Tolba et al. “A New Distribution for Modeling Data with Increasing Hazard Rate: A Case of COVID-19 Pandemic and Vinyl Chloride Data”. In: *Sustainability* 15.17 (2023), p. 12782.
- [43] Hal R Varian. “A Bayesian approach to real estate assessment”. In: *Studies in Bayesian econometrics and statistics in honor of Leonard J. Savage* (1975).
- [44] Yinghui Zhou et al. “On the implementation of a new version of the Weibull distribution and machine learning approach to model the COVID-19 data”. In: *Mathematical biosciences and engineering: MBE* 20.1 (2023), pp. 337–364.
- [45] Mi Zichuan et al. “A new extended-X family of distributions: properties and applications”. In: *Computational and Mathematical Methods in Medicine* 2020 (2020).